Journal of Solid State Chemistry 182 (2009) 2598–2601

Contents lists available at ScienceDirect

Journal of Solid State Chemistry

journal homepage: www.elsevier.com/locate/jssc

Doping induced magnetism in Co–ZnS nanoparticles

S. Sambasivam [a], D. Paul Joseph [b], J.G. Lin [a,*], C. Venkateswaran [b]

[a] Center for Condensed Matter Sciences, National Taiwan University, Taipei 10617, Taiwan
[b] Materials Science Centre, Department of Nuclear Physics, University of Madras, Guindy Campus, Chennai 600025, India

ARTICLE INFO

Article history:
Received 6 May 2009
Received in revised form
9 July 2009
Accepted 11 July 2009
Available online 17 July 2009

Keywords:
DMS
Nanoparticles
ESR
Magnetization

ABSTRACT

$Zn_{1-x}Co_xS$ nanoparticles with $x = 0$, 0.1, 0.2, and 0.3 were synthesized by the co-precipitation method using thiophenol as capping agent. The effect of Co doping on the structural, optical and magnetic properties are investigated. The X-ray diffraction patterns show single phase with cubic structure and the images of Transmission Electron Microscopy indicate an average particle size of 39 nm. Significant blue shift in the optical absorbing band edge was observed with increasing Co doping. In the Co doped samples, room-temperature (RT) magnetic hysteresis is observed and the magnetization reduces with increasing Co content. However, these samples show paramagnetic resonance instead of ferromagnetic resonance at both 300 and 80 K, suggesting that the origin of RT magnetization in these $Zn_{1-x}Co_xS$ nanoparticles involves with the frustration of antiferromagnetic interactions.

1. Introduction

ZnS nanocrystals are attractive for various optoelectronic applications, such as green light-emitting diodes, electro-optic field detectors, solar cells, lasers etc. [1–5] while the transition metal doped ZnS draw extensive attention as 'dilute magnetic semiconductor' (DMS) for spintronics applications [6–9]. In general, DMS behaves as a typical semiconductor, but its magnetization can be induced either by the exchange interactions mediated by free carriers or other exotic mechanism such as *F*-center ferromagnetic coupling [10]. In case of Mn doped DMS (such as $Cd_{1-x}Mn_xTe$ or $Zn_{1-x}Mn_xSe$), magnetism results solely from spins, showing the Brillouin-type paramagnetism [11]. However, the situation for Fe-doped DMS is completely different, in which the orbital momentum (d^6 configuration) is nonvanishing ($L = 2$, $S = 2$) and the ground state is a singlet closely next to the excited states. Consequently, a magnetic moment for the Fe ion can be induced by a magnetic field, which is the typical Van Vleck-type paramagnetism [12]. On the other hand, some DMS with the ferromagnetic long-range ordering at room temperature were reported [13–16]. It is now well understood that the observed ferromagnetism in various DMS can be either intrinsic or extrinsically from the segregated magnetic precipitates, depending on the method of synthesis and the concentration of transition metal. Few reports exist on studies of Co doped ZnS, ZnSe and CdSe bulk samples, suggesting that the strength of the antiferromagnetic (AFM) interactions in these systems is several times larger than their Mn-based counterparts [17,18]. In this study, we investigate the nature of Co-doping induced magnetism in ZnS nanoparticles. The strategy of using Co to replace Zn stems from the comparable ionic radii of Co^{2+} (0.72 Å) and Zn^{2+} (0.74 Å) and the same valency of these two ions. It is our attempt to avoid the segregation of Co ions due to the lattice distortion, maintain low defect density upon doping and enhance the solubility of substitution. The probe specifically chosen in this study is the electron spin resonance (ESR). Previous report on the ESR investigation of $Ga_{1-x}Mn_xAs$ reveal the fact that ESR is very sensitive to the local spin interactions [11], hence it provides an alternative probe to unravel the origin of magnetism in DMS.

2. Experiments

The $Zn_{1-x}Co_xS$ nanoparticles with $x = 0$, 0.1, 0.2 and 0.3 were prepared by the colloidal chemical co-precipitation method with zinc acetate and cobalt acetate as starting materials. The stoichiometric solution of 0.1 M is taken in a burette and added in drops with continuous stirring to a mixture of Na_2S (0.1 M)+50 mL of H_2O+2 mL of thiophenol+100 mL of methanol until the fine precipitates are formed. After the reactions are completed, the precipitates were then filtered out separately and peptized with de-ionized water and then calcined at 573 K/2 h in vacuum. The X-ray diffraction (XRD) patterns were obtained using Siefert 3003TT X-ray diffractometer. Particle size was estimated from the image of transmission electron microscopy (TEM). The optical absorption measurements were made in JASCO-V-560 spectrophotometer. The magnetization measurements were performed at 300 K in a vibrating sample magnetometer (Lakeshore 7404, USA). The Electron spin resonance (ESR) spectra of

* Corresponding author. Fax: +886 02 33665219.
E-mail address: jglin@ntu.edu.tw (J.G. Lin).

0022-4596/$ - see front matter © 2009 Elsevier Inc. All rights reserved.
doi:10.1016/j.jssc.2009.07.015

powder samples of all composition were recorded at 300 and 80 K using the Bruker EMX spectrometer operating at a frequency of 9.53 GHz.

3. Results and discussion

The X-ray diffraction patterns of $Zn_{1-x}Co_xS$ ($0 \le x \le 0.3$) samples annealed at 573 K/2 h in vacuum using CuK_α radiation in the range 20°–65° is shown in Fig. 1. The line broadening of the XRD patterns indicate the nanocrystalline nature of the samples. The XRD patterns of nanoparticles exhibit three broad peaks which could be indexed to the cubic structure of ZnS (JCPDS # 80-0020) in the entire range of composition studied and no extra peaks were found indicating the single phase, complete solubility of Co in ZnS. It is interesting to note that the Co doped ZnS nanoparticles synthesized using chemical capping agent yields cubic structure (JCPDS # 47-1655). Here again, thiophenol, the ligand seems to provide the surface capping effect and control the size of the nanoparticles to be in a narrow range. The average grain size of the nanoparticles obtained from FWHM intensity of the XRD peaks was in the range of 13–16 nm for $x = 0.0$, 0.1, 0.2 and 0.3, respectively. The EDAX measurements of $Zn_{1-x}Co_xS$ ($x = 0.1$, 0.2 and 0.3) respectively were measured using scanning electron microscope (Hitachi-S-3400N-SEM). A nominal variation in stoichiometry of Co of the synthesized $Zn_{1-x}Co_xS$ samples is observed (Table 1); however, this variation is around the desired stoichiometry. TEM measurements were also performed to study the morphology of the particles. Representative TEM micrograph of $Zn_{1-x}Co_xS$ ($x = 0.1$) is shown in Fig. 2. The particles were found to be isolated and nearly spherical in shape. The distribution plot fitted with a Gaussian profile is shown in the inset (right) of Fig. 2. The average particle size was estimated to be 39 nm. The particles observed in the TEM micrograph may be composed of a number of smaller crystallites [19,20]. The selected area electron diffraction (SAED) pattern of $Zn_{1-x}Co_xS$ ($x = 0.1$) is also shown in the inset (left) of Fig. 2. From the SAED rings, it is identified to have cubic structure with diffraction planes corresponding to (111), (220) and (311). No impurity phase could be identified.

The optical absorption spectra of $Zn_{1-x}Co_xS$ ($0 \le x \le 0.3$) nanoparticles is shown in Fig. 3. For bulk ZnS, the peak is expected at ~337 nm (bandgap, $E_g = 3.68$ eV), but the ZnS nanoparticles show two absorbance maxima between 300 and 400 nm in the near ultraviolet region. The band gap values corresponding to the maxima are 3.78 eV (328 nm) and 3.37 eV (367 nm). These two different absorbance maxima are illustrative of presence of groups of particles with two different sizes. $Zn_{1-x}Co_xS$ ($0.1 \le x \le 0.3$) were found to present only one absorbance maxima but slightly shifted to shorter wavelengths (blue shift) compared to un-doped ZnS. Introduction of Co systematically shifts the absorbance maxima towards shorter wavelength thereby increasing the band gap. The band gap values corresponding to the absorbance maxima with varying Co composition are presented in Table 1.

The magnetization data of $Zn_{1-x}Co_xS$ ($0.1 \le x \le 0.3$) (Fig. 4) annealed at 573 K/2 h in vacuum and measured at 300 K indicate hysteresis behavior. The preparation method does not involve any magnetic components and therefore we rule out the possibility of contamination from external magnetic impurities. XRD and

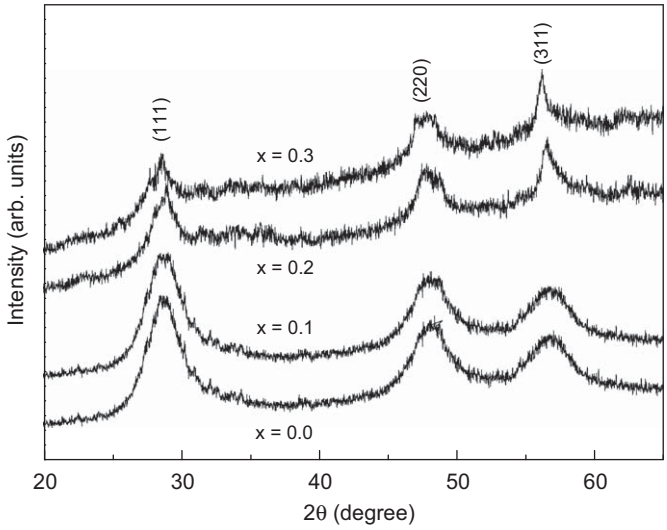

Fig. 1. XRD patterns of $Zn_{1-x}Co_xS$ with $x = 0.0$, 0.1, 0.2 and 0.3.

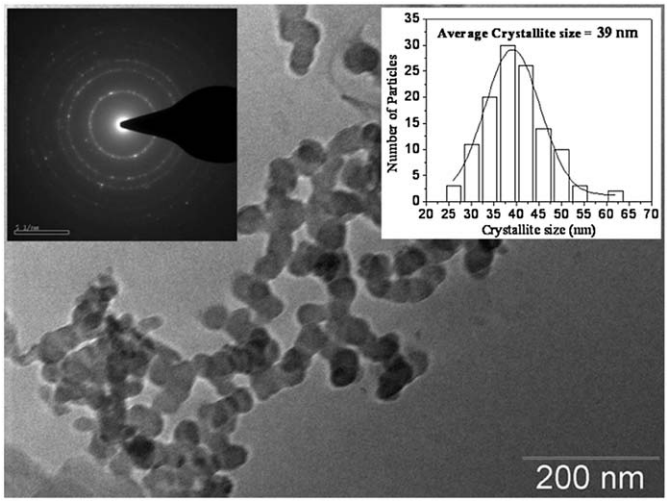

Fig. 2. TEM micrograph of $Zn_{0.9}Co_{0.1}S$ with the insets showing the corresponding SAED pattern (right) and the size distribution plot (left).

Table 1
Composition, energy gap, magnetic moment, g-values, line width (ΔH) and number of spins (N_s) of $Zn_{1-x}Co_xS$ ($x = 0.0$, 0.1, 0.2 and 0.3) nanoparticles are listed.

$Zn_{1-x}Co_xS$ sample	Co content (x) from EDAX	E_g (eV)	M_{Max} (μ_B/Co) at 300 K	g Value at 300 K	ΔH (Oe) at 300 K	g Value at 80 K	ΔH (Oe) 80 K	N_s at 80 K ($\times 10^{-3}$/ cm^{-3})
$Zn_{1-x}Co_xS$ ($x = 0$)	–	3.78 and 3.37	–	–	–	–	–	–
$Zn_{1-x}Co_xS$ ($x = 0.1$)	0.13	3.81	0.0693	1.944	6.4	2.008	20.6	3.48
$Zn_{1-x}Co_xS$ ($x = 0.2$)	0.19	3.85	0.0283	1.945	8.8	2.008	22.8	10.80
$Zn_{1-x}Co_xS$ ($x = 0.3$)	0.27	3.93	0.0144	1.944	9.4	2.007	24.5	17.58

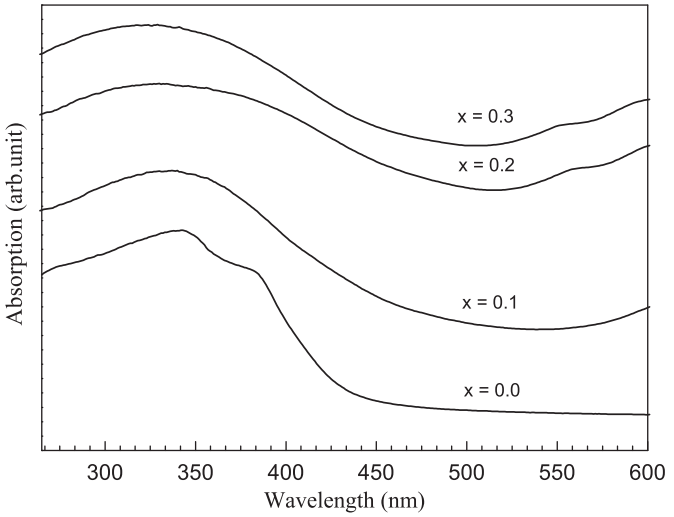

Fig. 3. Blue shift observed in the optical absorption spectra of $Zn_{1-x}Co_xS$ ($x = 0.0$, 0.1, 0.2 and 0.3) nanoparticles annealed at 573 K /2 h in vacuum. (For interpretation of the references to the color in this figure legend, the reader is referred to the web version of this article.)

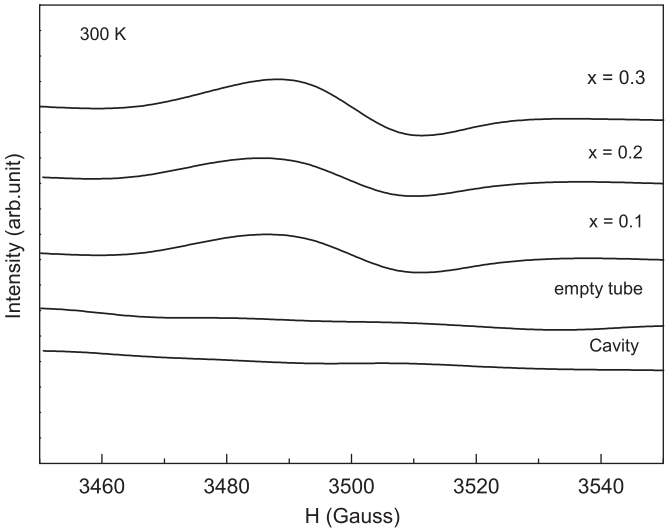

Fig. 5. ESR spectra at 300 K of the $Zn_{1-x}Co_xS$ nanoparticles with $x = 0.1$, 0.2 and 0.3.

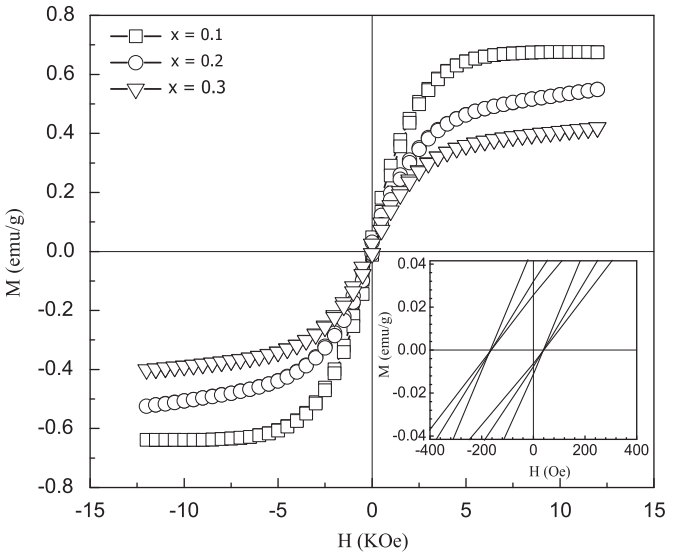

Fig. 4. Room temperature hysteresis loops for the $Zn_{1-x}Co_xS$ ($x = 0.1$, 0.2 and 0.3) nanoparticles, indicating a reduction of M_{Max} value. Inset shows the loop shift due to exchange bias effect.

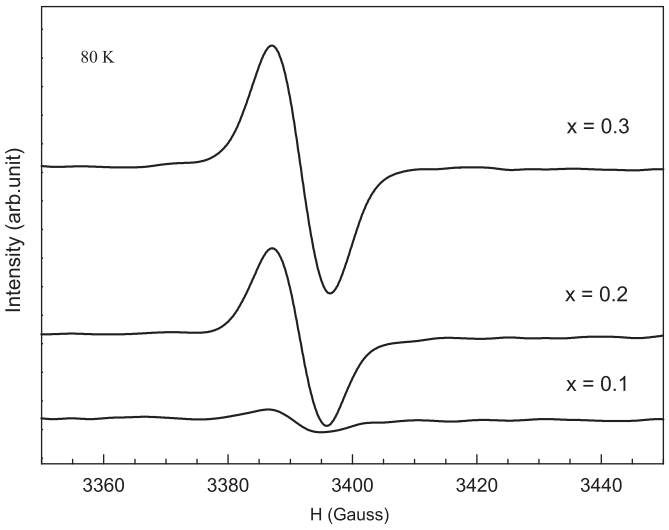

Fig. 6. ESR spectra at 80 K of the $Zn_{1-x}Co_xS$ nanoparticles with $x = 0.1$, 0.2 and 0.3.

SAED patterns show single phase within their detection limits. The small value of coercivity (H_C) (Table 1) indicates the soft magnetic behavior of the samples. No notable variation in coercivity is observed, in fact the coercivity is invariable with Co concentration. The loop of ($x = 0.1$) Co doped ZnS was found to be saturated, for the applied field of 1.5 T. For further increase in Co concentration, the value of maximum magnetization (M_{Max}) was found to decrease systematically and the loops also did not saturate. This interesting feature of systematic reduction in magnetization may be due to introduction of antiferromagnetic ordering with increasing 'Co' concentration as observed in the case of 'Co' doped ZnO [21–23]. In case of Co doped ZnO the sign of the magnetic interaction (ferromagnetic or antiferromagnetic) depend on the distance between Co atoms. In a random mixture of Zn and Co atoms, some Co atoms may be at shorter distances than others resulting in antiferromagnetic coupling; thus increase in Co content will reduce the Co–Co distances and may reinforce antiferromagnetic interactions. Hence, the reduction in magnetization may be due to competition between the antiferromagnetic and ferromagnetic ordering within the sample with increasing Co concentration. As supportive evidence, one could clearly observe the exchange bias effect [24] which is an interface interaction observed in a ferromagnetic–antiferromagnetic mixture. The exchange bias field (loop shift) towards negative field was around 63 Oe for the $Zn_{1-x}Co_xS$ ($0.1 \leq x \leq 0.3$) nanoparticles.

For further investigating on the nature of magnetic interactions, the ESR spectra of all the samples were taken at 300 and 80 K and are shown in Figs. 5 and 6 respectively. No resonant line is detected for pure ZnS sample; while single absorption line appears in the Co-doped samples. Both Figs. 5 and 6 show that the intensity (normalized to the weight) of ESR signal is enhanced with increasing Co-doping. The g-value can be determined based on the equation of $g = h\nu/\mu_B H_r$, where ν, μ_B and H_r are microwave frequency, Bohr magnetron and resonance

field respectively. As listed in Table 1, at both temperatures 300 and 80 K, the g value is independent of Co content and close to 2 for all doped samples, which is in contrast with the result for $Zn_{1-x}Co_xS$ ($g = 2.248$) single crystals [25]. Our finding implies that the type of field induced spin-response in our Co doped ZnS nanoparticles is paramagnetic while it is ferromagnetic in bulk form. Compared with the ESR data of Co doped TiO_2 [26], it is evident that the observed resonant line in our samples come from neither the direct Co^{2+}–Co^{2+} interaction nor the isolated Co^{2+} ions. It is interesting to note that the g value is slightly lower than 2 at 300 K, which is a signature of spin-fluctuation in an antiferromagnetic local field [27]. According to the integration and double-integration of ESR spectra, the line width (ΔH) and the relative number of effective spins (N_s) were calculated respectively and recorded in the Table 1. N_s increases with Co content, which can be interpreted as an increment of Co related effective spins. The value of ΔH is obtained as 6.4–9.4 Oe and 20.6–24.5 Oe for 300 and 80 K respectively, prevailing that the interaction between spins exists but is weak. Combining the data of magnetic hysteresis loops and the ESR spectra, it is suggested that the origin of room temperature magnetization in these $Zn_{1-x}Co_xS$ nanoparticles is stemmed from the frustration of antiferromagnetically coupled spins.

4. Conclusion

Co doped ZnS nanoparticles using thiophenol ligand were successfully synthesized. Based on the XRD patterns, the samples are single-phase with cubic structures. TEM micrographs indicate the average particle size to be 39 nm for the nearly spherical particles. Blue shift was observed in the optical absorption edge with increasing Co concentration. The Co doped samples show room temperature hysteresis loops, but the M_{Max} value was found to decrease due to coexistence of antiferromagnetic interaction with increasing Co concentration and tend to exhibit exchange bias with loop shift towards negative field. ESR data further suggest that the room temperature magnetization is not related to either the ferromagnetic exchange coupling of Co^{2+}–Co^{2+} or the isolated Co^{2+} ions. Instead, the magnetic response to the external field is likely associated with the frustration of antiferromagnetically correlated spins.

Acknowledgments

The authors acknowledge the financial support from the National Science Council of ROC under Grant nos. 96-2112-M-002-027-MY3. The author DPJ acknowledges the CSIR, Govt. of India for the award of Senior Research Fellowship (2007).

References

[1] L.E. Brus, Acc. Chem. Res. 23 (1990) 183.
[2] D. Kim, K.D. Min, J. Lee, J.H. Park, J.H. Chun, Mater. Sci. Eng. B 131 (2006) 13.
[3] Y. Wang, N. Herron, J. Phys. Chem. 95 (1991) 525.
[4] V.L. Colvin, M.C. Schlamp, A.P. Alivisatos, Nature 370 (1994) 354.
[5] R.N. Bharagava, J. Lumin. 70 (1996) 85.
[6] I. Sarkar, M.K. Sanyal, S. Kar, S. Biswas, S. Banerjee, S. Chaudhuri, S. Takeyama, H. Mino, F. Komori, Phys. Rev. B 75 (2007) 224409.
[7] S. Bhattacharya, D. Chakravorty, Chem. Phys. Lett. 444 (2007) 319.
[8] S. Yatsunenko, K. Swiatek, M. Godlewski, M. Froba, P.J. Klar, W. Heimbrodt, Opt. Mater. 30 (2008) 753.
[9] T. Kang, J. Sung, W. Shim, H. Moon, J. Cho, Y. Jo, W. Lee, B. Kim, J. Phys. Chem. 113 (2009) 5352.
[10] J.M.D. Coey, A.P. Douvalis, C.B. Fitzgerald, M. Venkatesan, Appl. Phys. Lett. 84 (2004) 1332.
[11] J. Schneider, U. Kaufmamm, W. Wilkening, M. Baeumler, F. Kohl, Phys. Rev. Lett. 59 (1987) 240.
[12] A. Twardowski, H.J.M. Swagten, W.J.M. de Jonge, M. Demimianiuk, Phys. Rev. B 44 (1991) 2220.
[13] K. Ueda, H. Tabata, T. Kawai, Appl. Phys. Lett. 79 (2001) 988.
[14] D. Paul Joseph, G. Senthil Kumar, C. Venkateswaran, Mater. Lett. 59 (2005) 2720.
[15] K.W. Liu, J.Y. Zhang, D.Z. Shen, B.H. Li, X.J. Wu, B.S. Li, Y.M. Lu, X.W. Fan, Thin Solid Films 515 (2007) 8017.
[16] S. Sambasivam, D. Paul Joseph, D. Raja Reddy, B.K. Reddy, C.K. Jayasankar, Mater. Sci. Eng. B 150 (2008) 125.
[17] T.M. Giebultowicz, P. Klosowski, J.J. Rhyne, T.J. Udovic, J.K. Furdyna, W. Giriat, Phys. Rev. B 41 (1990) 504.
[18] A. Lewicki, A.I. Schindler, J.K. Furdyna, W. Giriat, Phys. Rev. B 40 (1989) 2379.
[19] J.-S. Hu, L.-L. Ren, Y.-G. Guo, H.-P. Liang, A.-M. Cao, L.-J. Wan, C.-L. Bai, Angew. Chem. Int. Ed. 44 (2005) 1269.
[20] C. Bi, L. Pan, M. Xu, J. Yin, L. Qin, J. Liu, H. Zhu, J.Q. Xiao, Mater. Chem. Phys. 116 (2009) 363.
[21] B. Martinez, F. Sandiumenge, L. Balcells, J. Fontcuberta, F. Sibieude, C. Monty, J. Appl. Phys. 97 (2005) 10D311.
[22] B. Martinez, F. Sandiumenge, L. Balcells, J. Arbiol, F. Sibieude, C. Monty, Phys. Rev. B 72 (2005) 165202.
[23] Y. Wang, Y. Song, S. Yin, G. Yu, J. Miao, S. Yuan, Mater. Sci. Eng. B 131 (2006) 9.
[24] W.H. Meiklejohn, C.P. Bean, Phys. Rev. 102 (1956) 1413.
[25] F.S. Ham, G.W. Ludwig, G.D. Watkins, H.H. Woodbury, Phys. Rev. Lett. 5 (1960) 468.
[26] A. Manivanan, G. Glaspell, P. Dutta, M.S. Seehra, J. Appl. Phys. 97 (2005) 10D325.
[27] T.G. Kumary, J.G. Lin, J. Appl. Phys. 103 (2008) 053913.